Synthesis, characterization, crystal structures and magnetic properties of di- and polynuclear bis(μ-3-pyridin-2-yl-1,2,4-triazolato)copper(II) compounds containing *N*-methylimidazole, pyrazole or 4,4′-bipyridine as co-ligands

Petie M. Slangen, Petra J. van Koningsbruggen, Jaap G. Haasnoot*, Jacob Jansen, Syb Gorter and Jan Reedijk

Department of Chemistry, Gorlaeus Laboratories, Leiden University, P.O. Box 9502, 2300 RA Leiden (Netherlands)

Huub Kooijman, Wilberth J.J. Smeets and Anthony L. Spek

Bijvoet Center for Biomolecular Research, Vakgroep Kristal- en Structuurchemie, Utrecht University, Padualaan 8, 3584 CH Utrecht (Netherlands)

(Received February 8, 1993)

Abstract

A group of new compounds **1**–**5** of general formula $[Cu_2(pt)_2L_2(NO_3)_2(H_2O)_2](H_2O)_n$, with $n=1$, 2, 3 or 4 and L = *N*-methylimidazole, pyrazole, $\frac{1}{2}$ 4,4′-bipyridine, H_2O and *N*-butylimidazole, has been prepared and characterized spectroscopically and structurally. The synthesis, characterization, spectral and magnetic properties as well as crystal and molecular structures of [bis(μ-3-pyridin-2-yl-1,2,4-triazolato-*N′*,*N*1,*N*2)]-bis[(1-methylimidazole-*N*3)(nitrato)(aqua)copper(II)] tetrahydrate, $([Cu_2(pt)_2(Meim)_2(NO_3)_2(H_2O)_2](H_2O_4)_4$ (**1**), in which pt = 3-pyridin-2-yl-1,2,4-triazolato and Meim = *N*-methylimidazole, [bis(μ-3-pyridin-2-yl-1,2,4-triazolato-*N′*,*N*1,*N*2)]-bis[(pyrazole-*N*1)(nitrato)(aqua)copper(II)], $[Cu_2(pt)_2(Hpz)_2(NO_3)_2(H_2O)_2]$ (**2**) in which Hpz = pyrazole, and an unusual chain of dimers, *catena*-(μ-4,4′-bipyridine)[bis(μ-3-pyridin-2-yl-1,2,4-triazolato-*N′*,*N*1,*N*2)(nitrato)(aqua)copper(II))], $[Cu_2(pt)_2(4,4'\text{-bpy})(NO_3)(H_2O)_2](NO_3)(H_2O)_4$ (**3**) in which 4,4′-bpy = 4,4′-bipyridine, have been studied. Crystal structure data are as follows. **1**: $Cu_2N_{14}C_{22}H_{34}O_{12}$, $T=293$ K, triclinic, space group $P\bar{1}$, with $a=9.2685(6)$, $b=9.6897(6)$, $c=10.2313(4)$ Å, $\alpha=108.700(4)$, $\beta=97.884(4)$, $\gamma=95.396(5)°$, $Z=1$ and $V=852.75(8)$ Å^3. The least-squares refinement based on 2111 significant reflections ($I>2\sigma(I)$) converged to $R=0.0411$ and $R_w=0.0446$. **2**: $Cu_2N_{14}C_{20}H_{22}O_8$, $T=298$ K, monoclinic, space group $P2_1/c$, with $a=10.812(1)$, $b=13.750(1)$, $c=10.003(1)$ Å, $\beta=113.94(1)°$, $Z=2$ and $V=1359.1(2)$ Å^3. The least-squares refinement based on 1863 significant reflections ($I>2.5\sigma(I)$) converged to $R=0.0522$ and $R_w=0.0485$. **3**: $Cu_2N_{12}C_{24}H_{30}O_{12}$, $T=295$ K, monoclinic, space group $P2_1/c$, with $a=8.8802(11)$, $b=12.9975(8)$, $c=28.7208(19)$ Å, $\beta=92.970(7)°$, $Z=4$ and $V=3310.5(5)$ Å^3. The least-squares refinement based on 5100 significant reflections ($I>2\sigma(I)$) converged to $R=0.056$ and $R_w=0.051$. The structures of **1**, **2** and **3** consist of dinuclear units, in which the copper(II) ions are linked by two via N(1), N(2) bridging dehydronated Hpt ligands in the equatorial plane. Cu–N distances vary from 1.970(3) to 1.988(3) Å. All copper(II) ions are in a distorted octahedral environment, of which the equatorial plane around the copper atoms is formed by three donor atoms of the pt ligand and one donor atom of another ligand (Meim, Hpz or 4,4′-bpy). A water molecule and a monodentate nitrate anion occupy the axial positions. The Cu–Cu distances within the dinuclear unit are: **1**, 4.022(1); **2**, 3.9741(12); **3**, 4.0198(7) Å. The 4,4′-bpy ligand bridges the dinuclear units to form a ladder type chain, with a Cu–Cu distance measured over the 4,4′-bpy ligand of 11.1220(5) Å. The magnetic susceptibility data are interpreted on the basis of the spin Hamiltonian $\hat{H}=-2J[\hat{S}_{Cu1}\cdot\hat{S}_{Cu2}]$ and yielded **1**: $J=-47$ cm^{-1}, $g=2.14$, **2**: $J=-49$ cm^{-1}, $g=2.04$; **3**: $J=-51$ cm^{-1}, $g=2.14$; **4**: $J=-51$ cm^{-1}, $g=2.00$; **5**: $J=-51$ cm^{-1}, $g=2.07$. No interdimer interaction was found for **3**. The X-band powder EPR spectra recorded at various temperatures for all compounds are typical of a triplet state, with D values in the range 0.08–0.10 cm^{-1}.

Introduction

The magnetic properties of paramagnetic transition metal ions linked by diazine moieties have been the subject of intensive study over the past few years [1–8]. A particular class of ligands under study is formed by the 1,2,4-triazole derivatives containing N-donating chelating substituents [1–10]. A series of such dinuclear coordination compounds has been synthesized in which

*Author to whom correspondence should be addressed.

0020-1693/93/$6.00

the metal ions are linked in the equatorial coordination plane by two via N1, N2 bridging 1,2,4-triazole ligands [1–5]. The magnitude of the antiferromagnetic interactions between adjacent Cu(II) ions is related to the Cu–N–N angle [5]. The magnetic exchange is propagated via the $d(x^2-y^2)$ orbitals on the Cu(II) ions which interact with the σ orbitals of the nitrogens of the bridging ligand. The bridging mode of 3,5-bis(pyridin-2-yl)-1,2,4-triazolato [1, 2] (hereafter abbreviated as bpt) and 4-amino-3,5-bis(aminomethyl)-1,2,4-triazole [3, 4] (hereafter abbreviated as aamt) is fairly symmetrical with all Cu(1)–N(2)–N(1) and Cu(2)–N(1)–N(2) angles almost identical and in the range 132.9(8)–135.2(2)°, whereas for 3-pyridin-2-yl-1,2-4-triazolato [5] an asymmetric bridge with Cu–N–N of 139.8(3)° and 124.4(3)°/125.3(3)° has been found. These structural differences lead to a less efficient overlap of the magnetic orbitals situated on Cu(II) for the pt compound, which is reflected in the singlet–triplet energy gap. These are in the range of $-2J = 194$–236 cm^{-1} for the bpt [1, 2] and aamt [3, 4] copper(II) compounds and $-2J = 98$ cm^{-1} for $[Cu_2(pt)_2(SO_4)(H_2O)_3](H_2O)_3$ [5]. The main origin for this difference in bridging geometry is inherent to the nature of the triazole ligands. A regular bridging geometry is imposed by the use of the symmetrically substituted aamt and bpt. The monosubstituted pt, however, leads to asymmetric 1,2,4-triazole bridges. This also implies that in the pt compounds the fourth equatorial coordination site can vary. In fact in $[Cu_2(pt)_2(SO_4)(H_2O)_3](H_2O)_3$ [5] a monodentate coordinating sulfate and a water molecule have been found at this position. For the present study it was decided to vary systematically the ligand in this fourth coordination place, while keeping all other ligands the same. In this way subtle changes in the equatorial coordination sphere can be introduced and the influence on the bridging geometry and the magnetic properties can be studied in detail. In this respect it is mentioned that the magnitude of the interaction through a given bridging network can be tuned by modifying the nature of the terminal ligands, which – in some way – play the role of adjusting screws [11, 12]. In the present study we have selected water, two imidazoles, a pyrazole and a pyridine as co-ligands. Furthermore, with an appropriate ligand, the dinuclear units may be connected in an elegant way; for this we have selected the 4,4′-bipyridine ligand. In this article we wish to report on the crystal structures of three complexes containing pt and a co-ligand. The structures are discussed in relation to their magnetic susceptibility and EPR properties.

Experimental

Syntheses

Starting materials

Commercially available solvents and copper(II) nitrate trihydrate were used without further purification. The ligand Hpt was synthesized according to the method of Hage and co-workers [13, 14] from 2-cyanopyridine (Fluka A.G.), hydrazine hydrate (Janssen Chimica) and formic acid (J.T. Baker) as starting materials.

$[Cu_2(pt)_2(NO_3)_2(H_2O)_2](H_2O)_3$ (4)

2 mmol (0.27 g) of Hpt dissolved in a hot mixture of 10 ml of ethanol and 20 ml of water were added to 6 mmol (1.45 g) of $Cu(NO_3)_2 \cdot 3H_2O$ in 10 ml of water. The hot solution was filtered and after a few days the blue compound crystallized upon slow evaporation of the solvent at room temperature. *Anal.* Calc. for $[Cu_2(pt)_2(NO_3)_2(H_2O)_2](H_2O)_3$: Cu, 20.13; C, 26.63; H, 3.19; N, 22.18. Found: Cu, 19.47; C, 27.29; H, 2.99; N, 23.13%. UV–Vis spectroscopy: asymmetric band at 13.9×10^3 cm^{-1}. Yield = 65%.

$[Cu_2(pt)_2(Meim)_2(NO_3)_2(H_2O)_2](H_2O)_4$ (1)

As **4** but to this solution 6 mmol (0.49 g) of *N*-methylimidazole were added. *Anal.* Calc. for $[Cu_2(pt)_2(Meim)_2(NO_3)(H_2O)_2](H_2O)_4$: Cu, 15.62; C, 32.47; H, 4.21; N, 24.10. Found: Cu, 15.33; C, 33.21; H, 3.77; N, 25.01%. UV–Vis spectroscopy: asymmetric band at 16.1×10^3 cm^{-1}. Yield = 57%.

$[Cu_2(pt)_2(Hpz)_2(NO_3)_2(H_2O)_2]$ (2)

As **4** but 6 mmol (0.41 g) of pyrazole were added. A particular sample gave: *Anal.* Calc.: Cu, 17.42; C, 32.93; H, 3.04; N, 26.88. Found: Cu, 17.20; C, 33.06; H, 2.99; N, 27.45%. This is in accordance with the composition $[Cu_2(pt)_2(Hpz)_2(NO_3)_2(H_2O)_2](H_2O)$. From this batch a suitable crystal was selected for an X-ray structure determination. However, this crystal appeared to possess the composition $[Cu_2(pt)_2(Hpz)_2(NO_3)_2(H_2O)_2]$. In this paper, this compound is referred to as $[Cu_2(pt)_2(Hpz)_2(NO_3)_2(H_2O)_2]$. UV–Vis spectroscopy: asymmetric band at 16.0×10^3 cm^{-1}. Yield = 62%.

$[Cu_2(pt)_2(4,4'\text{-bpy})(NO_3)_2(H_2O)_2](H_2O)_4$ (3)

As **4** but 2 mmol (0.31 g) of 4,4′-bipyridine were added. *Anal.* Calc. for $[Cu_2(pt)_2(4,4'\text{-bpy})(NO_3)_2(H_2O)_2](H_2O)_4$: Cu, 15.77; C, 35.78; H, 3.75; N, 20.86. Found: Cu, 15.97; C, 35.59; H, 3.62; N, 21.03%. UV–Vis spectroscopy: asymmetric band at 15.9×10^3 cm^{-1}. Yield = 54%.

$[Cu_2(pt)_2(nBum)_2(NO_3)_2(H_2O)_2](H_2O)$ (5)

As **4** but 6 mmol (0.74 g) of *N*-butylimidazole were added. *Anal.* Calc. for $[Cu_2(pt)_2(nBuim)_2(NO_3)_2(H_2O)_2](H_2O)$: Cu, 15.06; C, 39.86; H, 4.78; N, 23.24. Found: Cu, 14.78; C, 40.18; H, 4.58; N, 23.79%. UV–Vis spectroscopy: asymmetric band at 16.1×10^3 cm^{-1}. Yield = 62%.

Physical measurements

C, H, N and Cu determinations were performed by the Microanalytical Laboratory of University College, Dublin, Ireland.

UV–Vis spectra were obtained on a Perkin-Elmer 330 spectrophotometer using the diffuse reflectance technique, with MgO as a reference.

X-band powder EPR spectra (variable temperature) were obtained on a Jeol RE2x electron spin resonance spectrometer using an ESR900 continuous-flow cryostat.

Magnetic susceptibilities were measured in the temperature range 10–300 K with a fully automized Manics DSM-8 susceptometer equipped with a TBT continuous-flow cryostat and a Drusch EAF 16 NC electromagnet, operating at *c.* 1.4 T. Data were corrected for magnetization of the sample holder and for diamagnetic contributions, which were estimated from the Pascal constants. Magnetic data were fitted to theoretical expressions by means of a Simplex routine [15], using a computer program written by R. Prins. All parameters (J, g and p) were varied independently during the fitting procedure. This routine minimizes the function $R = |\Sigma|\chi_{obs} - \chi_{calc}|^2 / |\Sigma\chi_{obs}|^2|^{1/2}$.

Crystallographic data collection and refinement of the structures

Crystal structure determination of 1

A blue crystal of approximate dimensions $0.20\times0.17\times0.065$ mm was used in the structure determination. Parameters of data collection and refinement are summarized in Table 1. The cell constants were determined at 293 K on an Enraf-Nonius CAD-4 automated diffractometer using graphite monochromated Cu Kα radiation from 23 reflections with $40 < \theta < 45°$ and ω–2θ scan type, scan angles $1.00 + 0.15$ tan $\theta°$, horizontal aperture 1.3–5.9 mm, vertical aperture 4.0 mm. Corrections for Lorentz and polarization effects. Relative transmission coefficients 0.702 to 1.260, $\mu = 21.84$ cm^{-1}. $2.0 < \theta < 65.0°$. h: -10 to 0; k: -11 to 11; l: -12 to 12. Standard reflections $-2\,0\,0$, $0\,1\,-1$. Decay of scattering power 4.67%. 3177 measured reflections, 2889 independent, $R_{int} = 0.0023$, 778 reflections with ($I < 2\sigma(I)$) were classified as unobserved. The structure was solved using direct methods. Least-squares refinement on F. All hydrogen atoms could be located in Fourier maps. Least-squares refinement of positional and non-hydrogen anisotropic thermal parameters; $S = 2.034$, $w = 1/\sigma(F)$, $R = 0.0411$, $R_w = 0.0446$, $(\Delta/\sigma)_{max} < 0.02$. The final difference synthesis revealed residual electron density between 0.13 and -0.17 e $Å^{-3}$ with a noise level of 0.11. Scattering factors and anomalous dispersion corrections were taken from the International Tables for X-ray Crystallography [16]. A Leiden University computer (IBM 3083) was used with MULTAN [17] and programs written or modified by S. Gorter, R.A.G. de Graaff and E.W. Rutten-Keulemans. The preparation of the illustrations was done with ORTEP [18]. Final fractional coordinates for non-hydrogen atoms are given in Table 2.

Crystal structure determination of 2

A blue, plate-shaped crystal of approximate dimensions $0.32\times0.18\times0.05$ mm was sealed in a Lindemann-glass capillary and transferred to an Enraf-Nonius CAD4-F diffractometer. Distance crystal to detector was 173 mm. Accurate unit-cell parameters and an orientation matrix were determined by least-squares refinement of 25 well-centred reflections (SET4) in the range $9.9 < \theta < 13.9°$ and ω–2θ scan type, scan angles $0.66 + 0.35$ tan $\theta°$, horizontal aperture 2.39 mm, vertical aperture 4.00 mm. Data set: h: -14 to 14; k: 0 to 17; l: -13 to 12. The unit-cell parameters were checked for the presence of higher lattice symmetry [19]. Crystal data and details on data collection and refinement are collected in Table 1. Data were corrected for L_p effects. Three periodically measured reference reflections ($-2\,0\,-2$, $-3\,-2\,2$, $2\,0\,2$) showed no significant linear decay (<1%) during 11 h of X-ray exposure time. $R_{int} = 0.0311$. An empirical absorption and extinction correction was applied (DIFABS [20], correction range 0.701–1.373). The structure was solved by automated direct methods (SHELXS86 [21]). Refinement on F was carried out by full-matrix least-squares techniques (SHELX76 [22]). Hydrogen atoms (including the pyrazole hydrogen H3) were included in the refinement on calculated positions (C, N–H = 0.98 Å) riding on their carrier atoms, except for the water hydrogen atoms H1 and H2, which were located on a difference Fourier map and subsequently included in the refinement. All non-hydrogen atoms were refined with anisotropic thermal parameters; the hydrogen atoms were refined with two overall isotropic thermal parameters with values of 0.05(2) and 0.065(7) $Å^2$ for the water hydrogen atoms and the other hydrogen atoms, respectively. Weights were introduced in the final refinement cycles. Convergence was reached at $R = 0.0522$. $(\Delta/\sigma)_{av} = 0.0329$ and $(\Delta/\sigma)_{max} = 0.376$ in final cycle. A final difference Fourier map showed no residual density outside -0.53 and 0.50 e $Å^{-3}$. Final positional parameters for non-hydrogen atoms are listed in Table 3. Neutral atom scattering factors were taken from Cromer and Mann [23], anomalous dispersion corrections from Cromer

TABLE 1 Crystal data and details of the structure determination for $[Cu_2(pt)_2(Meim)_2(NO_3)(H_2O)_2](H_2O)_4$ (**1**), $[Cu_2(pt)_2(Hpz)_2(NO_3)_2(H_2O)_2]$ (**2**), $[Cu_2(pt)_2(4,4'\text{-bpy})(NO_3)(H_2O)_2](NO_3)(H_2O)_4$ (**3**)

Compound	**1**	**2**	**3**
Chemical formula	$Cu_2N_{14}C_{22}H_{34}O_{12}$	$Cu_2N_{14}C_{20}H_{22}O_8$	$Cu_2N_{12}C_{24}H_{30}O_{12}$
Formula weight (g mol^{-1})	813.69	713.58	805.668
Crystal system	triclinic	monoclinic	monoclinic
Space group	$P\bar{1}$	$P2_1/c$	$P2_1/c$
a (Å)	9.2685(6)	10.812(1)	8 880(1)
b (Å)	9.6897(6)	13 750(1)	12.9975(8)
c (Å)	10.2313(4)	10.003(1)	28.721(2)
α (°)	108.700(4)	90	90
β (°)	97 884(4)	113.94(1)	92 970(7)
γ (°)	95.396(5)	90	90
V (Å^3)	852.75(8)	1359.1(2)	3310.5(5)
Z	1	2	4
Temperature (K)	293	298	295
$F(000)$ (electrons)	418	724	1648
ρ_{obs}	1.60	1.75	1 60
ρ_{calc}	1.58	1.74	1.62
λ (Å)	1.5418[a]	0.71073[b]	1.5418[a]
μ (cm^{-1})	21.84	16.4	22.29
No. unique data	2889	3111	6244
Scan type	ω–2θ	ω–2θ	ω–2θ
θ min.–max. (°)	2.0–65.0	1.48–27.5	2.50–70 0
Total no. data	3177	3719	6244
Observed data	2111 ($I>2\sigma(I)$)	1836 ($I>2$ 5$\sigma(I)$)	5100 ($I>2\sigma(I)$)
No. refined parameters	263	207	564
Final R[c]	0 0411	0.0522	0.056
Final R_w[d]	0 0446	0 0485	0.051
Weights	$1/\sigma^2(F)$	$1/[\sigma^2(F)+0.000256F^2]$	$1/\sigma^2(F)$
GOF[e]	2.034	1.55	2 342
Residual density: min., max. (e/Å^3)	−0.17, 0 13	−0.53, 0.50	−0.7, 0.8

[a]Graphite monochromated Cu Kα radiation [b]Graphite monochromated Mo Kα radiation [c]$R=(\Sigma(|F_{obs}|-|F_{calc}|)/\Sigma|F_{obs}|$. [d]$R_w=[\Sigma w(|F_{obs}|-|F_{calc}|)^2/\Sigma w|F_{obs}|^2]^{1/2}$. [e]$GOF=[\Sigma w(k|F_{obs}|-|F_{calc}|)^2/(NO-NV)]^{1/2}$.

and Liberman [24]. Geometrical calculations were performed with PLATON [25]. All calculations were performed on a DEC station 5000/125. The preparation of the illustrations was done with ORTEP [18]. Final fractional coordinates for non-hydrogen atoms are given in Table 3.

Crystal structure determination of 3

The intensities from a crystal of dimensions 0.15×0.18×0.30 mm were collected with an Enraf-Nonius CAD-4 diffractometer using graphite-monochromated Cu Kα radiation and ω–2θ scans. Parameters of data collection and refinement are summarized in Table 1. Preliminary scans indicated the crystal to be monoclinic with systematic absences $h0l$, $l\neq 2n$ and $0k0$, $k\neq 2n$, indicating space group $P2_1/c$. Two standard reflections, namely −1 2 −1 and 0 1 6, were measured with intervals of one hour. These reflections showed a radiation decrease of 6.15% during the 84 h of collection time, for which the intensities were corrected. Unit-cell parameters were determined by a least-squares algorithm using 25 reflections with $39\leqslant 2\theta\leqslant 42°$. The intensities were corrected for Lorentz and polarization effects. In order to get an estimate of the absorption, after the determination of the atomic positions the empirical absorption correction DIFABS [20] was applied. The positions of the copper atoms could be found using Patterson functions. With the program AUTOFOUR [26] we were able to locate the non-hydrogen atoms with the exception of some oxygen atoms. The position of the remaining atoms was determined by a Fourier synthesis. Three of the hydrogen atoms of water molecules could not be determined. One of the two nitrate groups appeared to be disordered. To overcome this problem two ions with the same centering nitrogen were introduced, whose occupations add to one. Subsequently, a full matrix least-squares refinement on F applying anomalous dispersion converged to $R=0.056$, $R_w=0.051$, $S=2.342$, max $\Delta/\sigma=0.056$. The reflection weights involved were $1/\sigma^2(F)$. The temperature factors of the hydrogen atoms were not refined and kept fixed at 0.035. The isotropic secondary-extinction coefficient [27] refined to $2.7(7)\times 10^{-6}$. The occupancies of the atoms O21, O22 and O23 refined to 0.48(3) and thus the occupancies of the atoms O21′, O22′ and O23′ are 0.52(3). Since the temperature factors of these oxygen

TABLE 2 Final coordinates and equivalent isotropic thermal parameters ($\times 10^3$ for Cu; $\times 10$ for C(16), C(34); $\times 10^2$ for all other atoms) of the non-hydrogen atoms of $[Cu_2(pt)_2(Meim)_2(NO_3)_2(H_2O)_2](H_2O)_4$ with e s.d s given in parentheses

Atom	x/a	y/b	z/c	B_{iso}[a] (Å^2)
Cu	0.0972(1)	0.1093(1)	0.3906(1)	3170(15)
N(1)	0.0898(3)	−0.1303(3)	0 5362(3)	307(9)
N(2)	0.1488(3)	−0.0479(3)	0.4655(3)	298(9)
N(4)	0.2846(3)	−0.2276(3)	0 4570(3)	375(9)
N(11)	−0.0814(3)	0 3172(3)	0 1297(3)	404(10)
N(13)	0.0474(3)	0.2365(3)	0.2782(3)	338(9)
N(31)	0.2893(3)	0.0699(3)	0.3140(3)	333(9)
N(5)	−0.1393(5)	−0.2064(5)	0.1212(4)	527(14)
C(3)	0 2637(4)	−0.1096(4)	0.4209(4)	304(10)
C(5)	0.1747(4)	−0 2362(4)	0.5278(4)	390(12)
C(12)	−0.0552(4)	0.1995(3)	0.1630(3)	365(11)
C(14)	0.0871(4)	0 3858(3)	0.3160(4)	454(14)
C(15)	0.0082(4)	0.4361(4)	0.2253(4)	476(14)
C(16)	−0.1909(8)	0.3174(7)	0 0109(6)	65(2)
C(31)	0 3476(3)	−0 0438(3)	0.3398(4)	319(10)
C(32)	0.4728(4)	−0.0892(4)	0.2924(4)	421(13)
C(33)	0.5395(4)	−0.0164(4)	0 2159(5)	517(15)
C(34)	0.4828(4)	0 0998(4)	0.1914(5)	51(2)
C(35)	0.3561(4)	0.1397(4)	0.2423(4)	430(13)
O(1)	−0.0210(6)	−0.1330(6)	0.1804(5)	129(2)
O(2)	−0.2080(4)	−0.1711(4)	0.0333(4)	722(13)
O(3)	−0.1822(9)	−0 3109(5)	0 1464(5)	136(3)
O(4)	0.2232(3)	0 3066(2)	0.5824(2)	492(9)
O(5)	0 4575(4)	0.4308(4)	0.0991(4)	831(14)
O(6)	0.4876(3)	−0.4318(3)	0.3950(4)	481(9)

[a] $B_{iso} = \frac{8}{3}\pi^2 \times$ (trace of orthogonalized U_{ij}).

atoms are rather high, a high degree of disorder is still observed. This is a common feature of the group, which can rotate freely around the nitrogen atom in the center. The final difference synthesis revealed residual electron densities between −0.7 and 0.8 e Å^{-3}. The highest peak may represent a partial water molecule because the distances to the neighbouring oxygen atoms are of the order of 2.8 Å. However, the peak height is too low for a whole atom. All calculations were performed with XTAL3.0 [28] unless stated otherwise. The scattering factors were taken from Cromer and Mann [23] and International Tables for X-ray Crystallography [16]. The preparation of the illustrations was done with ORTEP [18]. Final fractional coordinates for the non-hydrogen atoms are given in Table 4.

Results and discussion

Molecular structure of $[Cu_2(pt)_2(Meim)_2(NO_3)_2(H_2O)_2](H_2O)_4$ (1)

The molecular structure of the dinuclear unit is depicted in Fig. 1, whereas relevant bond length and bond angle information is given in Tables 5 and 6. The triclinic cell contains two dinuclear copper(II) units

TABLE 3. Final coordinates and equivalent isotropic thermal parameters of the non-hydrogen atoms of $[Cu_2(pt)_2(Hpz)_2(NO_3)(H_2O)_2]$ with e s d.s given in parentheses

Atom	x/a	y/b	z/c	U_{eq}[a] (Å^2)
Cu	0.86781(7)	−0.02860(5)	0 58646(8)	0.0291(2)
O(1)	0.6874(6)	0 0067(4)	0.3310(5)	0.076(2)
O(2)	0.6855(7)	0.1076(5)	0.1683(6)	0.095(3)
O(3)	0.5703(6)	0 1364(4)	0.2942(6)	0 077(2)
O(4)	1.0434(5)	−0.0579(3)	0.8230(5)	0.0391(16)
N(1)	1.0527(4)	−0.0975(3)	0.4317(5)	0.0326(17)
N(2)	0 9619(4)	−0.1081(3)	0.4914(5)	0.0268(16)
N(4)	1 0026(5)	−0.2551(3)	0.4243(5)	0.0363(18)
N(5)	0 6483(6)	0 0849(5)	0.2630(6)	0.053(2)
N(11)	0.7552(5)	0 0380(3)	0.6732(5)	0 0318(16)
N(12)	0.6409(5)	0.0853(4)	0.5949(6)	0.0512(19)
N(31)	0.7837(5)	−0.1619(3)	0.5905(5)	0.0295(16)
C(3)	0.9337(5)	−0.2030(4)	0 4852(6)	0 0289(17)
C(5)	1.0731(6)	−0 1866(4)	0.3929(6)	0.0365(19)
C(13)	0.5979(8)	0.1332(7)	0.6831(8)	0.091(4)
C(14)	0 6823(8)	0 1143(6)	0.8225(8)	0.070(3)
C(15)	0.7803(6)	0.0563(4)	0.8123(6)	0.040(2)
C(31)	0.8357(5)	−0 2341(4)	0.5395(6)	0.0306(17)
C(32)	0.7960(7)	−0.3303(4)	0.5395(7)	0.045(2)
C(33)	0.6988(7)	−0.3516(5)	0 5919(7)	0.052(3)
C(34)	0 6470(7)	−0.2768(5)	0.6438(7)	0.051(3)
C(35)	0.6916(6)	−0.1841(5)	0 6425(6)	0.039(2)

[a] $U_{eq} = \frac{1}{3}\Sigma_i\Sigma_j U_{ij} a^*_i a^*_j (\vec{a}_i \vec{a}_j)$.

and eight lattice water molecules. The cluster consists of two crystallographically dependent copper(II) ions linked together by the two dehydronated Hpt ligands. The anionic pt ligand acts as a planar dinucleating ligand, with N(1) and N(2) as bridging atoms between the copper(II) ions. This 1,2,4-triazole bridging mode via N1,N2 is quite well known in copper(II) coordination compounds [1–7]. The Cu–N(pyridine) distances are also significantly larger than the Cu–N(triazole) distances. The Cu–Cu distance within the dinuclear unit is 4.022(1) Å. The Cu atom is in a distorted octahedron, of which the equatorial coordination sphere is formed by the three donor atoms of the anionic pt ligand (Cu–N(1)′ = 1.983(3), Cu–N(2) = 1.981(3) and Cu–N(31) = 2.061(3) Å) and a coordinating nitrogen atom of the Meim ligand (Cu–N(13) = 1.981(3) Å). The axial ligands are a water molecule and a nitrate anion, which are located *trans* with respect to each other on the two copper atoms (Cu–O(4) = 2.327(1), Cu–O(1) = 2.639(5) Å). The N(2)–Cu–N(31) bite angle is 80.4(1)°, which is comparable to the angles found for mononuclear copper (II) compounds with the related ligand 4-amino-3,5-bis(pyridin-2-yl)-1,2,4-triazole (hereafter abbreviated as abpt), i.e. 80.1(1)° in $[Cu(abpt)_2(H_2O)](HSO_4)_2$ [9] and 80.5(2)° in $[Cu(abpt)_2(TCNQ)_2]$ [10] (TCNQ = 7,7′,8,8′-tetracyanoquinodimethane), although remarkably smaller than in the dinuclear $[Cu(bpt)(CF_3SO_3)(H_2O)]_2$ [2] with bite angles between

TABLE 4. Final coordinates and equivalent isotropic thermal parameters of the non-hydrogen atoms of $[Cu_2(pt)_2(4,4'\text{-bpy})(NO_3)(H_2O)_2](H_2O)_4$ with e s d s given in parentheses

Atom	*x/a*	*y/b*	*z/c*	U_{eq}[a] (Å^2)
Cu(1)	0 26209(6)	0 27770(5)	0.70575(2)	0 0440(3)
Cu(2)	0 02994(6)	0 27560(5)	0 58182(2)	0 0450(3)
C(11)	0 1644(5)	0.2520(3)	0.8686(1)	0 055(2)
C(12)	0 1402(5)	0 1704(4)	0.8381(1)	0 060(2)
C(13)	0 1674(5)	0 1824(3)	0.7917(1)	0.057(2)
C(15)	0 2454(6)	0 3491(4)	0 8040(1)	0.071(3)
C(16)	0 2192(6)	0 3424(4)	0.8509(1)	0 070(3)
C(3)	0.4403(4)	0 1922(3)	0 6383(1)	0.051(2)
C(5)	0.3391(5)	0 1868(4)	0 5717(1)	0 064(3)
C(3)′	−0.1472(4)	0 3643(3)	0.6488(1)	0 053(2)
C(5)′	−0 0433(5)	0.3721(4)	0 7152(1)	0 063(3)
C(31)	0 5419(4)	0.1855(3)	0.6804(1)	0 053(2)
C(32)	0 6842(5)	0 1456(3)	0.6815(2)	0 063(3)
C(33)	0.7704(5)	0 1470(4)	0.7231(2)	0.071(3)
C(34)	0 7085(5)	0 1883(4)	0.7619(2)	0 070(3)
C(35)	0 5648(5)	0 2252(4)	0 7581(1)	0 066(3)
C(31)′	−0 2458(5)	0 3726(3)	0 6069(1)	0.056(2)
C(32)′	−0.3871(5)	0 4164(4)	0.6054(2)	0 069(3)
C(33)′	−0.4707(6)	0.4174(4)	0 5635(2)	0.078(3)
C(34)′	−0 4118(6)	0.3753(4)	0.5247(2)	0 081(3)
C(35)′	−0 2674(5)	0.3346(4)	0.5287(2)	0 072(3)
N(5)	0 1844(8)	−0 0124(5)	0.6662(2)	0 104(4)
N(6)	0 1832(6)	0 5484(4)	0 5992(2)	0 081(3)
N(14)	0 2198(4)	0 2704(3)	0 7745(1)	0.061(2)
N(1)	0.2399(3)	0 2325(3)	0 5976(1)	0.057(2)
N(2)	0 3068(3)	0 2352(2)	0.64160(9)	0 054(2)
N(4)	0 4655(4)	0.1590(3)	0 5952(1)	0.066(2)
N(1)′	0.0517(3)	0.3175(3)	0 6896(1)	0 059(2)
N(2)′	−0 0179(4)	0 3144(2)	0.6464(1)	0 057(2)
N(4)′	−0 1676(4)	0 4028(3)	0.6912(1)	0.067(2)
N(31)	0.4796(3)	0.2246(3)	0 7184(1)	0 059(2)
N(31)′	−0 1853(4)	0 3328(3)	0 5688(1)	0 064(2)
O(4)	0.3229(4)	0.4398(3)	0 7051(1)	0.076(2)
O(5)	−0 0560(4)	0 1128(3)	0.5865(1)	0 079(2)
O(1)	0 5930(4)	0 5010(3)	0 7338(1)	0.093(3)
O(2)	−0.3233(4)	0.0451(4)	0.5482(2)	0 102(3)
O(3)	−0 4799(5)	−0 1366(4)	0.5320(1)	0 123(4)
O(6)	0 4014(7)	−0 2128(4)	0.6136(2)	0.170(5)
O(11)	0.1192(6)	0.0449(4)	0 6910(2)	0 146(5)
O(12)	0 1393(6)	−0 0311(4)	0 6267(2)	0 164(5)
O(13)	0.3133(7)	−0.0470(5)	0 6754(2)	0.156(5)
O(21)	0.102(3)	0 480(2)	0 601(1)	0 16(2)
O(22)	0 242(4)	0.589(1)	0 6320(6)	0.14(1)
O(23)	0.226(2)	0.575(1)	0 5597(5)	0 105(9)
C(11)′	0 1318(5)	0 2568(3)	0.4187(1)	0 056(2)
C(12)′	0.1596(5)	0.3457(3)	0 4442(1)	0 063(3)
C(13)′	0 1279(5)	0 3494(4)	0.4908(1)	0 064(3)
C(15)′	0 0376(5)	0 1844(4)	0 4880(1)	0.070(3)
C(16)′	0.0667(6)	0 1752(4)	0 4415(1)	0 069(3)
N(14)′	0 0677(4)	0 2693(3)	0.5128(1)	0 059(2)
O(21)′	0.122(3)	0.485(2)	0 5773(5)	0 13(1)
O(22)′	0 260(2)	0.609(1)	0.5844(9)	0 19(2)
O(23)′	0.155(2)	0 559(1)	0.6414(4)	0 106(9)

[a] $U_{eq} = \frac{1}{3}\Sigma_i\Sigma_j U_{ij} a^*_i a^*_j (\vec{a}_i \cdot \vec{a}_j)$

78.6(1) and 79.5(1)°. The pyridyl group is slightly twisted with respect to the 1,2,4-triazole ring. The dihedral angle between this ring and the triazole is only 3.7(2)°.

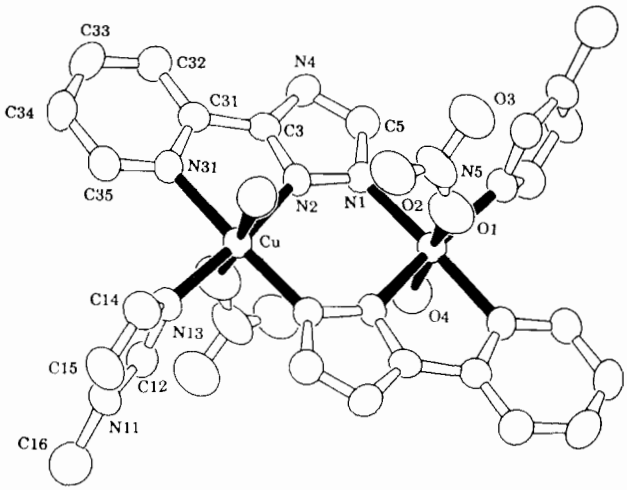

Fig. 1 The structure and atomic labeling of $[Cu_2(pt)_2(Meim)_2(NO_3)_2(H_2O)_2](H_2O)_4$ (**1**) Additional atoms are generated by the symmetry operation $-x, -y, 1-z$

TABLE 5. Bond distances (Å) for $[Cu_2(pt)_2(Meim)_2(NO_3)_2(H_2O)_2](H_2O)_4$, e s d.s in the last significant digits are given in parentheses

Cu–Cu′	4.022(1)
Cu–N(13)	1 981(3)
Cu–N(2)	1 981(3)
Cu–N(31)	2.061(3)
Cu–O(1)	2 639(5)
Cu–O(4)	2 327(1)
Cu–N(1)′	1 983(3)
N(13)–C(12)	1 334(1)
N(13)–C(14)	1 371(1)
N(1)–N(2)	1.362(4)
N(1)–C(5)	1 339(1)
N(2)–C(3)	1.334(5)
N(31)–C(35)	1.321(1)
N(31)–C(31)	1 354(2)
N(11)–C(12)	1 324(1)
N(11)–C(15)	1 360(1)
N(11)–C(16)	1 474(6)
N(4)–C(3)	1.332(4)
N(4)–C(5)	1 339(1)
N(5)–O(1)	1.213(6)
N(5)–O(2)	1 189(4)
N(5)–O(3)	1.170(6)
C(3)–C(31)	1 457(4)
C(14)–C(15)	1 342(1)
C(35)–C(34)	1.388(1)
C(32)–C(33)	1 377(1)
C(32)–C(31)	1.375(1)
C(34)–C(33)	1.364(1)

Primed atoms are generated by symmetry operation $-x, -y, 1-z$

The pt ligand bridges the copper atoms in an asymmetric mode, which is reflected in the Cu–N(2)–N(1) angle, which is 138.7(2)° and the Cu–N(1)′–N(2)′ angle, which is 125.8(2)°.

The Meim ligand makes an angle of 82.2(1)° with the pt ligand. This is probably due to steric hindrance.

TABLE 6 Bond angles (°) for $[Cu_2(pt)_2(Meim)_2(NO_3)_2(H_2O)_2](H_2O)_4$, e.s.d s in the last significant digits are given in parentheses

N(13)–Cu–N(2)	168 3(1)
N(13)–Cu–N(31)	93 0(1)
N(13)–Cu–O(1)	92 4(2)
N(13)–Cu–O(4)	93 1(1)
N(13)–Cu–N(1)′	90.7(1)
N(2)–Cu–N(31)	80 4(1)
N(2)–Cu–O(1)	77 5(2)
N(2)–Cu–O(4)	96 6(1)
N(2)–Cu–N(1)′	95.4(1)
N(31)–Cu–O(1)	84.3(2)
N(31)–Cu–O(4)	91.2(1)
N(31)–Cu–N(1)′	175 3(1)
O(1)–Cu–O(4)	173.1(1)
O(1)–Cu–N(1)′	92.7(2)
O(4)–Cu–N(1)′	91.4(1)
N(2)–N(1)–C(5)	104 8(3)
N(2)–N(1)–Cu′	125 8(2)
C(5)–N(1)–Cu′	128 9(2)
Cu–N(13)–C(12)	126 1(2)
Cu–N(13)–C(14)	127.5(2)
C(12)–N(13)–C(14)	105.2(3)
Cu–N(2)–N(1)	138 7(2)
Cu–N(2)–C(3)	114.4(2)
N(1)–N(2)–C(3)	106.1(3)
Cu–N(31)–C(35)	127.4(2)
Cu–N(31)–C(31)	113 9(2)
C(35)–N(31)–C(31)	118.7(3)
C(12)–N(11)–C(15)	108 0(3)
C(12)–N(11)–C(16)	125.3(4)
C(15)–N(11)–C(16)	126.7(3)
C(3)–N(4)–C(5)	101.8(3)
O(1)–N(5)–O(2)	117.5(6)
O(1)–N(5)–O(3)	121.3(6)
O(2)–N(5)–O(3)	121.2(6)
N(2)–C(3)–N(4)	113.5(3)
N(2)–C(3)–C(31)	117 9(3)
N(4)–C(3)–C(31)	128 6(3)
N(13)–C(12)–N(11)	110 7(3)
N(13)–C(14)–C(15)	109 6(3)
N(31)–C(35)–C(34)	122 3(3)
C(33)–C(32)–C(31)	118.4(3)
C(35)–C(34)–C(33)	118 6(3)
N(11)–C(15)–C(14)	106 5(3)
C(32)–C(33)–C(34)	120 0(3)
N(31)–C(31)–C(3)	112 9(3)
N(31)–C(31)–C(32)	122 0(3)
C(3)–C(31)–C(32)	125 2(3)
N(1)–C(5)–N(4)	113 8(3)
Cu–O(1)–N(5)	141.3(4)

Primed atoms are generated by symmetry operation: $-x$, $-y$, $1-z$

The structure is stabilized by a hydrogen bonding network, details of which are listed in Table 7.

Molecular structure of $[Cu_2(pt)_2(Hpz)_2(NO_3)_2(H_2O)_2]$ (2)

The molecular structure of the dinuclear cluster is depicted in Fig. 2, and relevant bond length and bond angle information is given in Tables 8 and 9. The monoclinic cell contains two dinuclear copper(II) units. The cluster consists of two crystallographically dependent copper(II) ions linked together by two dehydronated pt ligands. The asymmetric bridging geometry of the pt ligand is similar to that of **1** and $[Cu_2(pt)_2(SO_4)(H_2O)_3](H_2O)_3$ [5]. The Cu–Cu distance within the dinuclear unit is 3.9741(12) Å, which is the shortest Cu–Cu distance found for this type of double μ-N1,N2-triazole compound [1–5]. The coordination octahedron of the copper atom resembles that of the previous structure, with the exception that the fourth nitrogen atom in the equatorial plane is a nitrogen from the Hpz ligand (Cu–N(1) = 1.976(4), Cu–N(2) = 1.980(5), Cu–N(31) = 2.054(5), Cu–N(11) = 1.983(5) Å). The axial ligands, which are again a water molecule and a nitrate anion, are also coordinated in the same *trans* mode with distances Cu–O(1) = 2.554(5) and Cu–O(4) = 2.392(5) Å. The N(2)–Cu–N(31) bite angle is 80.5(2)°, which is comparable to that of **1**. The pyridyl group is also slightly twisted with respect to the 1,2,4-triazole ring. The dihedral angle between this ring and the triazole is only 2.1(3)°, which is slightly smaller than in **1**. Again the bridging mode is asymmetric with angles Cu′–N(1)–N(2) = 123.9(3)° and Cu–N(2)–N(1) = 139.6(3)° The angle between the pyrazole and the pt ligand is 83.3(3)°, about the same as in the case of Meim, and which is probably caused by steric hindrance. A hydrogen bonding network is further stabilizing the structure (see Table 10).

Molecular structure of $[Cu_2(pt)_2(4,4'\text{-bpy})(NO_3)_2(H_2O)_2](H_2O)_4$ (3)

The molecular and lattice structures of the chain of dinuclear copper(II) clusters are depicted in Figs. 3 and 4, respectively, whereas relevant bond length and bond angle information is given in Tables 11 and 12. The monoclinic cell contains two dinuclear copper(II) units and eight lattice water molecules. Unlike the structures **1** and **2**, two crystallographic independent distorted octahedrally coordinated copper(II) atoms are present in this structure, which differ slightly in their coordination spheres. The pt bridging mode is similar to those found in all other copper(II) pt structures, **1**, **2** and in ref. 5. The Cu(1)–Cu(2) distance within the dinuclear unit is 4.0198(7) Å, which is similar to the related structures. The dinuclear units are bridged by 4,4′-bpy molecules to form a chain. The Cu(1)–Cu(2) distance measured over the bridging 4,4′-bpy molecules is 11.1220(5) Å, which is comparable to the 11.106(2) Å for $[Cu_2(dien)_2(4,4'\text{-bpy})(ClO_4)_2](ClO_4)_2$ (in which dien is diethylenetriamine) [29]. The 4,4′-bpy pyridyl rings are twisted 38.9° with respect to each other, this is in contrast with the dihedral angle of 0° in $[Cu_2(dien)_2(4,4'\text{-bpy})(ClO_4)_2](ClO_4)_2$ and 3.7° in

TABLE 7. Interatomic distances (Å) and angles (°) for the hydrogen bonding interactions in $[Cu_2(pt)_2(Meim)_2(NO_3)_2(H_2O)_2](H_2O)_4$, e.s.d.s in the last significant digits are given in parentheses

D–H···A	D–H	H···A	D···A	D–H···A
O(4)–H1(O4)···O(3)[1]	0.8870(0)	1.961(5)	2.840(5)	170.3(2)
O(4)–H2(O4)···O(6)[2]	0.9594(0)	1.830(4)	2.784(4)	172.7(1)
O(5)–H1(O5)···O(2)[3]	0.9779(0)	2.171(6)	3.062(6)	150.8(1)
O(5)–H2(O5)···O(5)[4]	0.8763(0)	2.043(5)	2.918(7)	176.7(2)
O(6)–H1(O6)···N(4)	0.8993(0)	1.967(4)	2.842(4)	164.0(1)
O(6)–H2(O6)···O(5)[5]	0.9212(0)	1.987(5)	2.851(5)	155.6(1)
O(6)–H2(O6)···O(6)[6]	0.9212(0)	1.990(5)	2.856(7)	166.5(2)

Atoms marked with a number are generated by symmetry operations: [1] $-x, -y, 1-z$; [2] $1-x, -y, 1-z$; [3] $-x, -y, -z$; [4] $1-x, 1-y, -z$; [5] $x, -1+y, z$; [6] $1-x, -1-y, 1-z$.

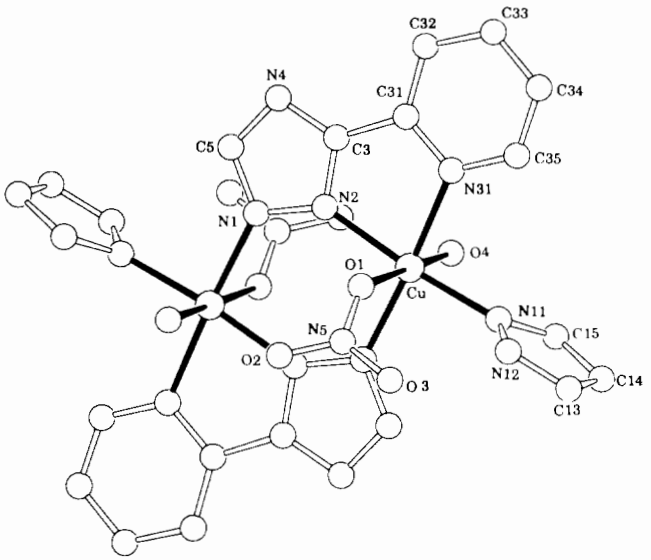

Fig. 2. The structure and atomic labeling of $[Cu_2(pt)_2(Hpz)_2(NO_3)_2(H_2O)_2]$ (2). Additional atoms are generated by the symmetry operation $2-x, -y, 1-z$.

TABLE 8. Bond distances (Å) for $[Cu_2(pt)_2(Hpz)_2(NO_3)_2(H_2O)_2]$, e.s.d.s in the last significant digits are given in parentheses

Cu–Cu′	3.9741(12)		
Cu–O(1)	2.554(5)	N(4)–C(5)	1.327(8)
Cu–O(4)	2.392(5)	N(11)–N(12)	1.334(8)
Cu–N(2)	1.980(5)	N(11)–C(15)	1.329(7)
Cu–N(11)	1.983(5)	N(12)–C(13)	1.346(11)
Cu–N(31)	2.054(5)	N(31)–C(31)	1.340(7)
Cu–N(1)′	1.976(4)	N(31)–C(35)	1.333(9)
O(1)–N(5)	1.251(8)	C(3)–C(31)	1.438(8)
O(3)–N(5)	1.234(9)	C(13)–C(14)	1.346(11)
O(2)–N(5)	1.211(9)	C(14)–C(15)	1.363(11)
N(1)–N(2)	1.348(7)	C(31)–C(32)	1.391(8)
N(1)–C(5)	1.330(7)	C(32)–C(33)	1.383(11)
N(2)–C(3)	1.336(7)	C(33)–C(34)	1.370(10)
N(4)–C(3)	1.344(8)	C(34)–C(35)	1.365(10)

Primed atoms are generated by the symmetry operation $2-x, -y, 1-z$.

TABLE 9. Bond angles (°) for $[Cu_2(pt)_2(Hpz)_2(NO_3)_2(H_2O)_2]$; e.s.d.s in the last significant digits are given in parentheses

O(1)–Cu–O(4)	177.6(2)	O(1)–N(5)–O(2)	120.1(7)
O(1)–Cu–N(2)	87.54(19)	O(3)–N(5)–O(2)	121.9(7)
O(1)–Cu–N(11)	89.7(2)	Cu–N(11)–N(12)	123.7(4)
O(1)–Cu–N(31)	91.42(19)	Cu–N(11)–C(15)	130.1(4)
O(1)–Cu–N(1)′	85.74(19)	N(12)–N(11)–C(15)	105.6(5)
O(4)–Cu–N(2)	91.48(18)	N(11)–N(12)–C(13)	110.0(6)
O(4)–Cu–N(11)	91.54(19)	Cu–N(31)–C(31)	113.3(4)
O(4)–Cu–N(31)	90.59(17)	Cu–N(31)–C(35)	128.3(4)
O(4)–Cu–N(1)′	92.18(18)	C(31)–N(31)–C(35)	118.3(5)
N(2)–Cu–N(11)	172.62(19)	N(2)–C(3)–N(4)	112.6(5)
N(2)–Cu–N(31)	80.5(2)	N(2)–C(3)–C(31)	117.5(5)
N(2)–Cu–N(1)′	96.50(19)	N(4)–C(3)–C(31)	129.9(5)
N(11)–Cu–N(31)	92.8(2)	N(1)–C(5)–N(4)	113.9(6)
N(11)–Cu–N(1)′	90.11(19)	C(13)–C(14)–C(15)	104.9(7)
N(31)–Cu–N(1)′	175.96(19)	N(12)–C(13)–C(14)	108.6(8)
Cu–O(1)–N(5)	131.3(4)	N(11)–C(15)–C(14)	110.8(6)
N(2)–N(1)–C(5)	105.5(4)	N(31)–C(31)–C(3)	114.3(5)
N(2)–N(1)–Cu′	123.9(3)	N(31)–C(31)–C(32)	121.8(6)
C(5)–N(1)–Cu′	130.7(4)	C(3)–C(31)–C(32)	123.9(6)
Cu–N(2)–N(1)	139.6(3)	C(31)–C(32)–C(33)	118.9(6)
Cu–N(2)–C(3)	114.2(4)	C(32)–C(33)–C(34)	118.4(6)
N(1)–N(2)–C(3)	106.2(4)	C(33)–C(34)–C(35)	119.8(7)
C(3)–N(4)–C(5)	101.9(4)	N(31)–C(35)–C(34)	122.7(6)
O(1)–N(5)–O(3)	118.1(6)		

′ = symmetry operation $2-x, -y, 1-z$.

TABLE 10. Interatomic distances (Å) and angles (°) for the hydrogen bonding interactions in $[Cu_2(pt)_2(Hpz)_2(NO_3)_2(H_2O)_2]$; e.s.d.s in the last significant digits are given in parentheses

D–H···A	D–H	H···A	D···A	D–H···A
O(4)–H(1)···N(4)[1]	0.79(7)	2.08(7)	2.863(6)	171(8)
O(4)–H(2)···O(2)[2]	0.74(8)	2.26(8)	2.98(1)	167(7)
N(12)–H(3)···O(1)	0.980(8)	2.419(8)	3.077(8)	124.0(6)
N(12)–H(3)···O(3)	0.980(8)	1.976(8)	2.874(8)	151.3(6)

Atoms marked with a number are generated by symmetry operations: [1] $x, -0.5-y, 0.5+z$; [2] $2-x, -y, 1-z$.

$[Cu(dien)(4,4'\text{-bpy})(H_2O)](ClO_4)_2$ [29]. The equatorial plane of the octahedron around Cu(1) is formed by the three donor atoms of the anionic pt ligand

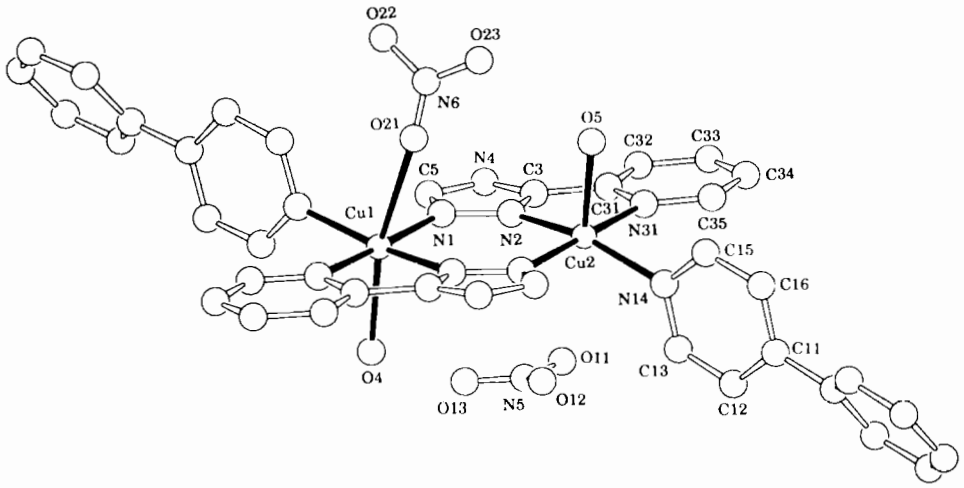

Fig 3. The structure and atomic labeling of $[Cu_2(pt)_2(4,4'\text{-bpy})(NO_3)_2(H_2O)_2](H_2O)_4$ (3)

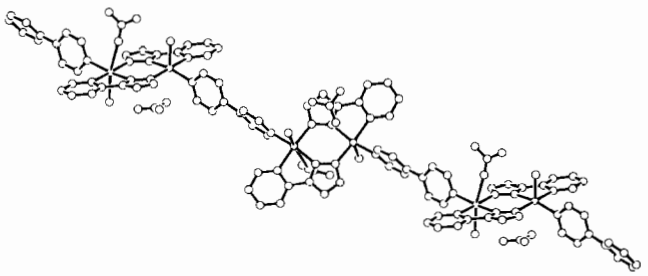

Fig. 4. The structure of $[Cu_2(pt)_2(4,4'\text{-bpy})(NO_3)_2(H_2O)_2](H_2O)_4$ (3) showing the linear chain structure.

(Cu(1)–N(1)′ = 1.970(3), Cu(1)–N(2) = 1.983(3), Cu(1)–N(31) = 2.066(3) Å) and one donor atom of the 4,4′-bpy molecule (Cu(1)–N(14) = 2.031(3) Å). The apical position is occupied by a coordinated water molecule (Cu(1)–O(4) = 2.175(4) Å). A nitrate anion is at a very long distance (Cu(1)–O(11) = 3.300(6) Å). Cu(2) has a similar coordination geometry with the exception that the nitrate is coordinating to the copper atom (Cu(1)–O(21) = 2.78(2) Å) and with slightly different bond lengths (and angles) (Cu(2)–N(1) = 1.978(3), Cu(2)–N(2)′ = 1.988(3), Cu(2)–N(31)′ = 2.067(3), Cu(2)–N(14)′ = 2.031(3) Å). The axial water molecule is *trans* to the water molecule bonded to Cu(1) (Cu(2)–O(2) = 2.255(4) Å). The cquatorial planes of the Cu(1) and Cu(2) coordination sphere make an angle of only 2.09(9)°. The N(2)–Cu(1)–N(31) and N(2)′–Cu(2)–N(31)′ bite angles are 80.8(1) and 80.6(1)°, respectively. These are in the same range found for the other copper(II) pt structures [5]. The pt pyridyl group is slightly twisted with respect to the 1,2,4-triazole ring. The dihedral angle between this ring and the triazole is 3.1(2)°, which is in the same range as the previous structures [5]. The via N1,N2 1,2,4-triazole bridging mode is a rather unusual asymmetric one, which is reflected in the Cu(1)–N(2)–N(1) and Cu(2)–N(2)′–N(1)′ angles, which are 140.0(2) and 138.7(2)°, respectively, and the Cu(1)–N(1)′–N(2)′ and Cu(2)–N(1)–N(2) angles, which are 126.0(2) and 124.3(2)°, respectively. In contrast to the above described dinuclear pt copper(II) compounds, the two ligands are not in a plane, since the least-squares plane through

TABLE 11 Bond distances (Å) for $[Cu_2(pt)_2(4,4'\text{-bpy})(NO_3)_2(H_2O)_2](H_2O)_4$; e.s.d s in the last significant digits are given in parentheses

Cu(1)–Cu(2)	4.0198(7)	C(34)–C(35)	1 362(7)
Cu(1)–N(14)	2 031(3)	C(35)–N(31)	1 337(5)
Cu(1)–N(2)	1 983(3)	C(31)′–C(32)′	1.376(6)
Cu(1)–N(1)′	1 970(3)	C(31)′–N(31)′	1.346(5)
Cu(1)–N(31)	2 066(3)	C(32)′–C(33)′	1.381(7)
Cu(1)–O(4)	2.175(4)	C(33)′–C(34)′	1 367(8)
Cu(2)–N(1)	1.978(3)	C(34)′–C(35)′	1 386(7)
Cu(2)–N(2)′	1.988(3)	C(35)′–N(31)′	1.332(5)
Cu(2)–N(31)′	2 067(3)	N(5)–O(11)	1.201(8)
Cu(2)–O(2)	2 255(4)	N(5)–O(12)	1.207(8)
Cu(2)–N(14)′	2.031(3)	N(5)–O(13)	1.245(9)
C(11)–C(12)	1.384(6)	N(6)–O(21)	1.15(2)
C(11)–C(16)	1.380(6)	N(6)–O(22)	1.18(2)
C(12)–C(13)	1.376(5)	N(6)–O(23)	1.27(2)
C(13)–N(14)	1.340(6)	N(6)–O(21)′	1.15(2)
C(15)–C(16)	1.383(6)	N(6)–O(22)′	1.14(2)
C(15)–N(14)	1.340(6)	N(6)–O(23)′	1.26(1)
C(3)–C(31)	1.473(5)	N(1)–N(2)	1 368(4)
C(3)–N(2)	1 318(5)	N(1)′–N(2)′	1.360(4)
C(3)–N(4)	1.338(5)	O(21)–O(21)′	0 71(3)
C(5)–N(1)	1.323(5)	O(21)–O(23)′	1 61(3)
C(5)–N(4)	1.330(5)	O(22)–O(22)′	1.41(3)
C(3)′–C(31)′	1.455(5)	O(22)–O(23)′	0.92(3)
C(3)′–N(2)′	1 324(5)	O(23)–O(21)′	1.59(3)
C(3)′–N(4)′	1 339(5)	O(23)–O(22)′	0.88(3)
C(5)′–N(1)′	1 348(5)	C(11)′–C(12)′	1.385(6)
C(5)′–N(4)′	1.332(5)	C(11)′–C(16)′	1 388(6)
C(31)–C(32)	1.365(6)	C(12)′–C(13)′	1.383(6)
C(31)–N(31)	1.349(5)	C(13)′–N(14)′	1.342(6)
C(32)–C(33)	1.384(6)	C(15)′–C(16)′	1.380(6)
C(33)–C(34)	1.377(7)	C(15)′–N(14)′	1.332(6)

TABLE 12. Bond angles (°) for $[Cu_2(pt)_2(4,4'\text{-bpy})(NO_3)_2(H_2O)_2](H_2O)_4$, e.s.d.s in the last significant digits are given in parentheses

N(14)–Cu(1)–N(2)	161.1(1)
N(14)–Cu(1)–N(1)′	91.1(1)
N(14)–Cu(1)–N(31)	91.8(1)
N(14)–Cu(1)–O(4)	96.4(1)
N(2)–Cu(1)–N(1)′	95.1(1)
N(2)–Cu(1)–N(31)	80.8(1)
N(2)–Cu(1)–O(4)	101.5(1)
N(1)′–Cu(1)–N(31)	174.7(1)
N(1)′–Cu(1)–O(4)	88.6(1)
N(31)–Cu(1)–O(4)	95.5(1)
N(1)–Cu(2)–N(2)′	95.9(1)
N(1)–Cu(2)–N(31)′	174.7(1)
N(1)–Cu(2)–O(2)	92.2(1)
N(1)–Cu(2)–N(14)′	90.7(1)
N(2)′–Cu(2)–N(31)′	80.6(1)
N(2)′–Cu(2)–O(2)	95.3(1)
N(2)′–Cu(2)–N(14)′	167.2(1)
N(31)′–Cu(2)–O(2)	92.0(1)
N(31)′–Cu(2)–N(14)′	92.1(1)
O(2)–Cu(2)–N(14)′	95.4(1)
Cu(1)–N(14)–C(13)	118.9(3)
Cu(1)–N(14)–C(15)	123.1(3)
Cu(1)–N(2)–C(3)	114.2(2)
Cu(1)–N(2)–N(1)	140.0(2)
Cu(1)–N(1)′–C(5)′	128.5(3)
Cu(1)–N(1)′–N(2)′	126.0(2)
Cu(1)–N(31)–C(31)	113.7(2)
Cu(1)–N(31)–C(35)	129.1(3)
Cu(2)–N(14)′–C(13)′	121.1(3)
Cu(2)–N(14)′–C(15)′	121.1(3)
Cu(2)–N(1)–C(5)	130.2(3)
Cu(2)–N(1)–N(2)	124.3(2)
Cu(2)–N(2)′–C(3)′	113.6(2)
Cu(2)–N(31)–C(31)′	113.4(2)
Cu(2)–N(31)′–C(35)′	128.5(3)
Cu(2)–N(2)′–N(1)′	138.7(2)
C(12)–C(11)–C(16)	117.7(4)
C(11)–C(12)–C(13)	119.8(4)
C(12)–C(13)–N(14)	122.4(4)
C(16)–C(15)–N(14)	122.5(4)
C(11)–C(16)–C(15)	119.5(4)
C(31)–C(3)–N(2)	118.7(3)
C(31)–C(3)–N(4)	127.9(3)
N(2)–C(3)–N(4)	113.5(3
N(1)–C(5)–N(4)	113.9(3)
C(31)′–C(3)′–N(2)′	118.7(3)
C(31)′–C(3)′–N(4)′	128.4(4)
N(2)′–C(3)′–N(4)′	122.9(3)
N(1)′–C(5)′–N(4)′	113.7(3)
C(3)–C(31)–C(32)	124.7(4)
C(3)–C(31)–N(31)	112.5(3)
C(32)–C(31)–N(31)	122.8(3)
C(31)–C(32)–C(33)	119.1(4)
C(32)–C(33)–C(34)	118.5(4)
C(33)–C(34)–C(35)	119.0(4)
C(34)–C(35)–N(31)	123.4(4)
C(3)′–C(31)′–C(32)′	124.5(4)
C(3)′–C(31)′–N(31)′	113.2(3)
C(32)′–C(31)′–N(31)′	122.3(4)
C(31)′–C(32)′–C(33)′	118.7(4)
C(32)′–C(33)′–C(34)′	119.6(5)
C(33)′–C(34)′–C(35)′	118.5(5)
C(34)′–C(35)′–N(31)′	122.7(4)
C(13)–N(14)–C(15)	118.0(3)
C(5)–N(1)–N(2)	105.1(3)
C(3)–N(2)–N(1)	105.7(3)
C(3)–N(4)–C(5)	101.8(3)
C(5)′–N(1)′–N(2)′	104.2(3)
C(3)′–N(2)′–N(1)′	107.0(3)
C(3)′–N(4)′–C(5)′	102.2(3)
C(31)–N(31)–C(35)	117.2(3)
C(31)′–N(31)′–C(35)′	118.2(4)
C(12)′–C(11)′–C(16)′	117.1(3)
C(11)′–C(12)′–C(13)′	120.1(4)
C(12)′–C(13)′–N(14)′	122.2(4)
C(16)′–C(15)′–N(14)′	123.1(4)
C(11)′–C(16)′–C(15)′	119.6(4)
C(13)′–N(14)′–C(15)′	117.8(3)
O(11)–N(5)–O(12)	122.4(7)
O(11)–N(5)–O(13)	124.3(6)
O(12)–N(5)–O(13)	112.6(6)
O(21)–N(6)–O(22)	125(2)
O(21)–N(6)–O(23)	118(2)
O(22)–N(6)–O(23)	117(1)

all atoms of one pt ligand makes an angle of 3.5(1)° with the one of the pt on the opposite side of the plane. The coordinated pyridyl ring of 4,4′-bpy makes an angle of 87.7(1)° with the pt ligand, again most likely due to steric effects. The structure is stabilized further by an important network of hydrogen bonds, details of which are listed in Table 13.

Ligand field spectroscopy

The ligand field band centered at 13.9×10^3 cm^{-1} for **4** is in agreement with the presence of a CuN_3O_3 chromophore, whereas the values of 15.9×10^3 to 16.1×10^3 cm^{-1} for the other compounds are consistent with the presence of CuN_4O_2 chromophores [30].

Magnetic properties

The magnetic susceptibilities have been recorded in the 10–300 K temperature region. For all five compounds a behaviour for an antiferromagnetically coupled copper(II) dinuclear compound is found with a maximum in the χ versus T curve between 90 to 100 K. Figure 5 shows the magnetic behaviour of $[Cu_2(pt)_2(Meim)_2(NO_3)_2(H_2O)_2](H_2O)_4$ (**1**). The magnetic data for all compounds have been fitted to the modified Bleaney and Bowers expression for $S=1/2$ dimers [31].

$$\chi_m = \frac{2N\beta^2g^2}{kT}\,[3+\exp(-2J/kT)]^{-1}(1-p)+\chi_p p \qquad (1)$$

in which $2J$ is the singlet–triplet energy gap defined by the phenomenological spin Hamiltonian with quantum spin operators, $\hat{S}_1$ and $\hat{S}_2$

TABLE 13. Interatomic distances (Å) and angles (°) for the hydrogen bonding interactions in $[Cu_2(pt)_2(4,4'\text{-bpy})(NO_3)_2(H_2O)_2](H_2O)_4$; e s d.s in the last significant digits are given in parentheses

D–H· · A	D–H	H· · ·A	D· ·A	D–H· · ·A
O(5)–H(402) · ·O(22)	0 77(5)	2.08(5)	2 925(17)	161(4)
O(5)–H(402)· · ·O(23)′	0.77(5)	1.93(5)	2 774(16)	164(4)
O(5)–H(401)· · O(1)	0.77(5)	1.87(5)	2 519(5)	165(5)
O(1)–H(101)· · ·O(13)	0.91(4)	1.86(4)	2.769(6)	171(4)
O(1)–H(102)· · ·N(24)	0.97(5)	1 85(4)	2.813(5)	172(4)
O(4)–H(502) O(2)	0.65(5)	2.07(5)	2 710(5)	162(6)
O(4)–H(501)· O(12)	0.95(4)	1.89(4)	2.764(7)	151(3)
O(2)–H(201)· N(14)	0 67(5)	2 15(5)	2.792(6)	164(5)
O(2)–H(202) · ·O(3)	1.01(4)	1.76(5)	2.768(7)	171(3)
O(3)–H(301)· · ·O(6)	0.85(5)	1.98(5)	2 799(7)	162(4)
O(6)–H[a]· ·O(13)			2.924(8)	
O(6)–H[a]· · ·O(22)			3.00(2)	
O(6)–H[a]· O(22)′			2.742(18)	

[a]The position of these hydrogen atoms could not be determined.

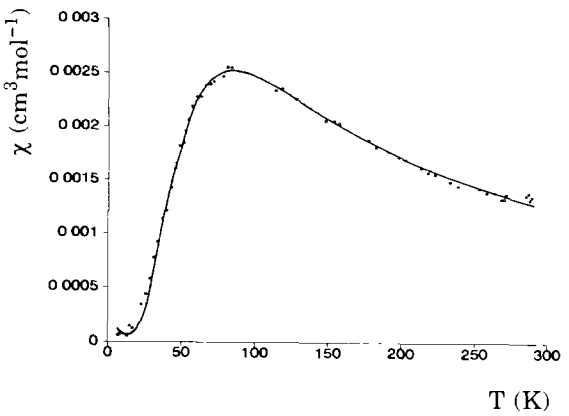

Fig. 5. χ vs. T curve for $[Cu_2(pt)_2(Meim)_2(NO_3)_2(H_2O)_2](H_2O)_4$ (**1**). The solid line represents the calculated curve ($J = -47$ cm^{-1} and $g = 2.14$).

$$\hat{H} = -2J(\hat{S}_1 \cdot \hat{S}_2) \qquad (2)$$

In formula (1) N, g, β, k and T have their usual meanings. The parameter p denotes the percentage of paramagnetic impurity present in the sample. The parameters for which the best fit has been obtained are given in Table 14. The magnetic superexchange pathway in double μ-N1,N2 triazole compounds is propagated as follows. In these compounds the unpaired electron of the copper(II) ion occupies a magnetic orbital of $d(x^2-y^2)$ symmetry, which is pointing towards the coordinating triazole nitrogen atoms. Consequently, a considerable electron delocalization may take place over these nitrogens and magnetic superexchange interaction becomes possible via mainly the σ-orbitals of the triazole ligand. Changes in the bridging geometry of the ligand are therefore likely to influence directly the efficiency of the exchange pathway. If the exchange parameter J calculated for the present compounds is compared to these of the symmetric dinuclear doubly N(1),N(2) 1,2,4-triazole bridged copper(II) compounds, it is seen that in the latter case the absolute value of J is significantly larger and J is in the range of -97 to -118 cm^{-1} [1–4]. Comparison of the angles involving the copper atom and the nitrogen atoms of the bridging network reveals a relationship between these angles and the magnitude of the J value. It is seen that a more symmetric bridging mode with the Cu(1)–N(2)–N(1) and Cu(2)–N(1)–N(2) angles close to 135°, as observed in the bpt [1, 2] and aamt [3, 4] compounds, allows a larger interaction than the more asymmetric bridging mode with a Cu(1)–N(2)–N(1)

TABLE 14. Magnetic and EPR parameters of $[Cu_2(pt)_2L_2(NO_3)_2(H_2O)_2](H_2O)_n$ ($n = 1$, 2, 3 or 4; L = *N*-methylimidazole, pyrazole, $\frac{1}{2}$ 4,4-bipyridine, H_2O and *N*-butylimidazole)

Compound	Magnetic parameters			EPR parameters	
	J (cm^{-1})	g	p	g	$g_{1/2}$
$[Cu_2(pt)_2(Meim)_2(NO_3)_2(H_2O)_2](H_2O)_4$ (**1**)	−48	2.14	2.0×10^{-3}	2.12	4 17
$[Cu_2(pt)_2(Hpz)_2(NO_3)_2(H_2O)_2]$ (**2**)	−49	2.04	3.7×10^{-3}	2.15	4.15
$[Cu_2(pt)_2(4,4'\text{-bpy})(NO_3)_2(H_2O)_2](H_2O)_4$ (**3**)	−51	2.14	2.5×10^{-2}	2.13	4.14
$[Cu_2(pt)_2(NO_3)_2(H_2O)_2](H_2O)_3$ (**4**)	−51	2.00	1.8×10^{-3}	2.15	4.16
$[Cu_2(pt)_2(nBuim)_2(NO_3)_2(H_2O)_2](H_2O)$ (**5**)	−51	2 07	4.9×10^{-3}	2 16	4.18

angle of 138.7(2) to 140.0(2)° and a Cu(2)–N(1)–N(2) angle of 123.9(3) to 126.0(2)°, which is observed in the present series of compounds [5]. This must be caused by the extent of overlap between the $d(x^2-y^2)$ orbitals and the σ-orbitals of the nitrogen atoms. The more these orbitals are directed towards each other the larger the overlap and therefore the antiferromagnetic interaction.

The influence of a change in the equatorial coordination sphere of Cu(II) does not have a considerable effect on the magnitude of the isotropic magnetic exchange. This is unlike in the case of the dinuclear μ-oxalato copper(II) compounds, where the magnitude of the magnetic interaction via the oxalate bridge can be tuned by modifying the nature of the terminal ligands [11, 12]. In that case the co-ligands cause a change in the coordination geometry of the copper(II) ions, whereby the orientation of the magnetic orbitals is changed. In the present series of pt copper(II) compounds the coordination octahedra around the copper(II) ions do not change significantly, in spite of the presence of co-ligands, and the magnetic orbitals remain in the plane of the bridging 1,2,4-triazole ligands. Therefore, for all compounds similar isotropic magnetic exchange parameters are found, as seen in Table 14.

No magnetic coupling could be observed between copper(II) ions which are linked via the 4,4′-bpy ligand. Apparently, the distance of 11.1220(5) Å is too long to allow magnetic exchange interaction. This is in agreement with the results obtained for $[Cu_2(dien)_2(4,4'\text{-bpy})(ClO_4)_2](ClO_4)_2$ [29], where also a very small (if any at all) coupling was found over the 4,4′-bpy ligand.

Representative X-band powder EPR spectra, measured at various temperatures, are presented in Fig. 6. The spectra are all typical for a triplet spin state and the normal feature for a Cu(II) dimer, the $\Delta m_s = 2$ signal, is observed [32]. The D values are in the range 0.08–0.10 cm^{-1}. The EPR parameters are listed in Table 14. The spectra show a decrease in intensity upon cooling, again characteristics for antiferromagnetic coupling between the copper(II) ions [32].

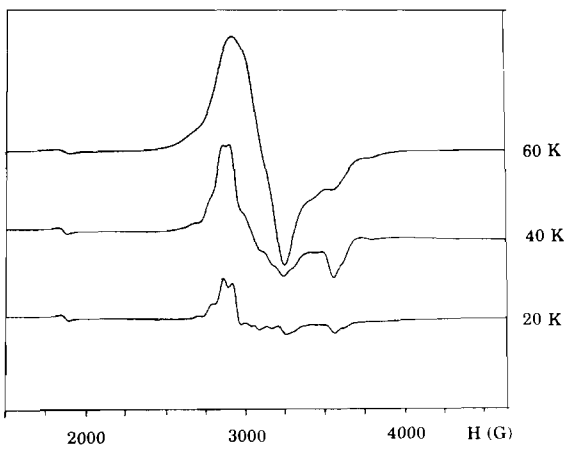

Fig. 6. X-band powder EPR spectra of $[Cu_2(pt)_2(Hpz)_2(NO_3)_2(H_2O)_2]$ (**2**) at 60, 40 and 20 K

Conclusions

The polynuclear bis(μ-3-pyridin-2-yl-1,2,4-triazolato)copper(II) nitrate compounds represent a unique class of compounds in which the monodentate coordinating ligands H_2O, *N*-methylimidazole, pyrazole, *N*-butylimidazole and 4,4′-bipyridine can occupy the remaining equatorial coordination position. It is evident that the co-ligands to be incorporated in the crystal lattice are by far not limited to the above mentioned ones. By the choice of the appropriate co-ligand these dinuclear copper(II) units can even be linked, as has been shown in the 4,4′-bipyridine compound, which is also the first linear chain reported with this co-ligand. Apparently, this linkage is only possible with longer ligand systems. For example, with pyrazole or 1,3-pyrazine such a linkage is not possible, since a too close vicinity of the copper(II) dimers is prohibited by steric hindrance.

Supplementary material

Tables of anisotropic thermal parameters, positional and thermal parameters for hydrogen atoms, selected least-squares planes, tables of calculated and observed structure factors of **1** and **3** may be obtained from author J.G.H. upon request.

Further details of the structure determination of **2**, including atomic coordinates, bond lengths and angles, thermal parameters and a thermal motion ellipsoid plot (9 pages) may be obtained from author A.L.S. upon request.

Acknowledgements

The authors thank the 'Werkgroep Fundamenteel Materialen Onderzoek' (W.F.M.O.) for financial support. Dr J.P. Cornelissen is acknowledged for helpful discussions. This work was supported in part (A.L.S and W.J.J.S.) by the Netherlands Foundation of Chemical Research (SON) with financial aid from the Netherlands Foundation for Scientific Research (NWO).

References

1 A Bencini, D Gatteschi, C. Zanchini, J G. Haasnoot, R. Prins and J Reedijk, *J. Am Chem Soc, 109* (1987) 2926.
2 R Prins, P.J M.W.L. Birker, J G Haasnoot, G.C. Verschoor and J. Reedijk, *Inorg. Chem, 24* (1985) 4128.
3 W.M.E van Oudenniel, R A.G. de Graaff, J.G Haasnoot, R Prins and J Reedijk, *Inorg. Chem, 28* (1989) 1128
4 P.J. van Koningsbruggen, J.G. Haasnoot, R.A G. de Graaff, J. Reedijk and S. Slingerland, *Acta Crystallogr, Sect C, 48* (1992) 1923
5 P.M Slangen, P.J. van Koningsbruggen, K. Goubitz, J G Haasnoot and J.Reedijk, *Inorg Chim Acta,* (1993) in press
6 P J. van Koningsbruggen, D. Gatteschi, R.A.G. de Graaff, J.G. Haasnoot, J. Reedijk and C. Zanchini, in preparation.
7 R. Prins, R A.G de Graaff, J.G Haasnoot, C. Vader and J. Reedijk, *J Chem. Soc, Chem Commun,* (1986) 1430.
8 A. Bencini, D. Gatteschi, C. Zanchini, J.G Haasnoot, R. Prins and J. Reedijk, *J Am Chem. Soc, 109* (1987) 2926.
9 P J van Koningsbruggen, K. Goubitz, J G. Haasnoot and J. Reedijk, to be submitted.
10 J P. Cornelissen, J.H. van Diemen, L.R. Groeneveld, J.G. Haasnoot, A.L. Spek and J Reedijk, *Inorg Chem, 31* (1992) 198.
11 O Kahn, in D. Gatteschi, O Kahn and R.D. Willett (eds.), *Magneto-Structural Correlations in Exchange Coupled Systems,* NATO Advanced Study Institute Series, Vol, C140, Reidel, Dordrecht, Netherlands, 1984
12 O. Kahn, *Angew Chem, Int. Ed Engl, 24* (1985) 834.
13 B.E Buchanan, R. Wang, J.G. Vos, R. Hage, J.G. Haasnoot and J. Reedijk, *Inorg Chem 29* (1990) 3263
14 R. Hage, *Ph D Thesis*, Leiden University, Netherlands, 1991
15 J.A Nelder and R. Mead, *Computer J, 7* (1965) 308
16 *International Tables for X-ray Crystallography,* Vol. IV, Kynoch, Birmingham, UK, 1974, p 55.
17 G. Germain, P. Main and M.M. Woofson, *Acta Crystallogr, Sect A, 27* (1971) 368.
18 C.K. Johnson, *ORTEP, Rep ORNL-3794,* Oak Ridge National Laboratory, TN, 1965
19 A.L. Spek, *J Appl Crystallogr, 21* (1988) 578
20 N. Walker and D. Stuart, *Acta Crystallogr, Sect A, 39* (1983) 158.
21 G.M. Sheldrick, *SHELXS86,* program for crystal structure determination, University of Gottingen, Germany, 1986.
22 G M. Sheldrick, *SHELX76,* program for crystal structure determination, University of Cambridge, UK, 1976.
23 D.T. Cromer and J.B. Mann, *Acta Crystallogr., Sect. A, 24* (1968) 321.
24 D.T. Cromer and D. Liberman, *J Chem Phys., 53* (1970) 1891.
25 A.L Spek, *Acta Crystallogr, Sect. A, 46* (1990) C34.
26 A J. Kinneging and R.A G. de Graaff, *J Appl Crystallogr, 17* (1984) 364.
27 A C. Larson, *Acta Crystallogr., 23* (1967) 644.
28 S.R. Hall and J.M. Stewart (eds), *XTAL3 0 User's Manual,* Universities of Western Australia and Maryland, 1990
29 M. Julve, M. Verdaguer, J. Faus, F. Tinti, J. Moratal, A. Monge and E. Gutiérrez-Puebla, *Inorg Chem., 26* (1987) 3520.
30 B.J. Hathaway and D.E. Billing, *Coord Chem Rev, 5* (1970) 143.
31 B. Bleaney and K.D. Bowers, *Proc R. Soc London, Ser. A, 214* (1952) 451.
32 A. Abragam and B. Bleaney, *Electron Paramagnetic Resonance of Transition Ions,* Oxford University Press, London, 1970.